Dielectronic-recombination rates for some ions of the lithium isoelectronic sequence

L. J. Roszman
Atomic and Plasma Radiation Division, National Bureau of Standards, Gaithersburg, Maryland 20899
(Received 15 January 1986)

The total dielectronic-recombination rates for Ne^{7+}, Ar^{15+}, Fe^{23+}, and Kr^{33+}, all members of the lithium isoelectronic sequence, are computed in the nonrelativistic, single-configuration, *LS*-coupling, frozen-core, corona model approximation. Comparison is made with other calculations, and differences are noted and analyzed. Analytic formulas for interpolating the total dielectronic-recombination rates for other members of the lithium isoelectronic sequence are given.

I. INTRODUCTION

Dielectronic recombination is a most significant recombination process for ions in hot plasmas at low and high densities. Because of its dominance in the low-density regime, dielectronic recombination is the most important recombination mechanism for heavy-ion impurities in the contained, high-temperature plasmas used in magnetic fusion-energy research. It has a significant impact on the ionization balance, the impurity transport, and the energy loss by the plasma through the line spectra of the impurity ions.[1,2] Similar considerations apply in certain astrophysical plasmas.[3]

The work reported in this paper consists of a series of calculations of the dielectronic recombination rates of initial ions which are members of the lithium isoelectronic sequence. The final, recombined, ions are, of course, members of the beryllium isoelectronic sequence. Environmental effects are ignored, i.e., the ions are treated as isolated with the effects of external fields and the plasma density ignored.

The atomic model and the corresponding calculational techniques are described in Secs. II and III. Section IV contains the results computed using the model and techniques described in Secs. II and III and contains comparisons with other detailed calculations. Comparison with the results of the Burgess-Merts analytic formula,[1,4] a discussion of the scaling properties of dielectronic-recombination rate coefficients, and a parametrization of the current results are presented in Sec. V. The region of accuracy of the atomic model is discussed and conclusions are made in Sec. VI.

II. ATOMIC MODEL

When the autoionizing resonances of an ion contained in a plasma are narrow and isolated from each other, the dielectronic-recombination rate coefficients of the ion, unperturbed by external fields or the plasma density, from some initial continuum state $|i\varepsilon\rangle$ through a particular autoionizing state $|j\rangle$ into a particular bound state $|k\rangle$ can be computed from the following equation:[5–7]

$$\alpha(i;j;k)=\frac{4\pi^{3/2}a_0^3}{2T^{3/2}g_i}\frac{A_a(j;i\varepsilon_j)A_r(j;k)}{\sum_{i'}A_a(j;i'\varepsilon_j)+\sum_{k'}A_r(j;k')}e^{-\varepsilon_j/T}. \tag{1}$$

The autoionization rate from the autoionizing state $|j\rangle$ into the continuum state $|i\varepsilon_j\rangle$ is denoted by $A_a(j;i\varepsilon_j)$, and the radiative rate from the autoionizing state $|j\rangle$ into the bound state $|k\rangle$ is denoted by $A_r(j;k)$. The energy of the autoionizing state $|j\rangle$ with respect to the first ionization limit of the recombined ion is ε_j, and a_0 is the Bohr radius. The quantity g_i is the statistical weight of the initial unrecombined ion state (without consideration of the continuum orbital). The units of the temperature of the plasma electrons, T, and of the autoionization energy are rydbergs. A Maxwellian distribution of the energy of the plasma electrons has been assumed. The "total" rate of dielectronic recombination is obtained by summing over all possible initial continuum, intermediate autoionizing, and bound final states.

The continuum orbitals and the autoionizing and bound Rydberg orbitals are computed in the frozen-core Hartree-Fock approximation. For the case of the lithium isoelectronic sequence, which is considered in this study, the configurations of the core structures are

$$1s^22s,\ 1s^22p\ , \tag{2}$$

$$1s^23s,\ 1s^23p,\ 1s^23d\ , \tag{3}$$

$$1s^24s,\ 1s^24p,\ 1s^24d,\ 1s^24f\ . \tag{4}$$

The core structures $1s2s^2$ and $1s2s2p$ are not considered in this study. The plasma conditions under which these states must be included are noted in Sec. VI. The wave functions associated with the core configurations of Eqs. (2)–(4) are computed using a self-consistent-field (SCF) Hartree-Fock computer code based upon the representation of the orbitals of the core wave function as a series of analytic Slater-type orbitals.[8,9] The configuration-averaged approximation is sufficient for the generation of these wave functions. A Hartree-Fock equation is solved for each bound and autoionizing Rydberg orbital of interest with the Hartree-Fock exchange interaction approximated by a local-exchange term based upon the Hartree-plus-statistical-exchange (HX) method of Cowan.[10] This approximate Schrödinger equation for a Rydberg orbital

with principal quantum number n, angular momentum l, and energy ε_{nl} has the form

$$\left[-\frac{d^2}{dr^2}+\frac{l(l+1)}{r^2}+V_d-\varepsilon_{nl}\right]P_{nl}(r)=0\ , \tag{5}$$

where the potential term V_d is defined by the following:

$$V_d=-\frac{2z}{r}+\sum_i (N_i-\delta_{nn_i}\delta_{ll_i})\frac{2}{r}Y_0(n_il_i,n_il_i/r) -0.6\left[\frac{\rho'}{\rho'+0.5/(n-l)}\right]\left[\frac{24}{\pi}\rho'\right]^{1/3} \tag{6}$$

with the altered electron density ρ' given by

$$\rho'=\frac{1}{4\pi r^2}\sum_i N_i(P_{n_il_i})^2\ . \tag{7}$$

The quantity $Y_0(nl,nl/r)$ is defined in the usual manner,

$$Y_0(nl,nl/r)=\int_0^r dr'r'[P_{nl}(r')]^2 +r\int_r^\infty dr'r'^{-1}[P_{nl}(r')]^2\ . \tag{8}$$

The Rydberg orbitals are computed in a center-of-gravity approximation, also.

The continuum orbital is computed in a configuration-averaged, distorted-wave approximation with the Hartree-Fock exchange interaction replaced with a spherically averaged version of the semiclassical exchange introduced by Riley and Truhlar.[11] The Schrödinger equation for the continuum orbital has the form

$$\left[-\frac{d^2}{dr^2}+\frac{l(l+1)}{r^2}+V_c-\varepsilon\right]P_{\varepsilon l}(r)=0\ , \tag{9}$$

where the potential term is given by

$$V_c(r)=-\frac{2z}{r}+\frac{2}{r}\sum_i N_iY_0(n_il_i,n_il_i/r) -0.5\left[\frac{2}{r}\sum_i N_iY_0(n_il_i,n_il_i/r)-\frac{2z}{r}-\varepsilon\right] -0.5\left[\left[\frac{2}{r}\sum_i N_iY_0(n_il_i,n_il_i/r) -\frac{2z}{r}-\varepsilon\right]^2+4\alpha^2\right]^{1/2} \tag{10}$$

with the local electron charge density defined by

$$\alpha^2=\frac{1}{r^2}\sum_i N_i[P_{n_il_i}(r)]^2\ . \tag{11}$$

The differential equations for the bound orbitals, Eq. (5), and for the continuum orbitals, Eq. (9), are solved using the Kutta δ^2 method[12] with the energy iteration determined by the Ridley method.[13] The Kutta δ^2 method and the Ridley method are very stable and well suited to unmonitored production computations, though the Ridley method is slightly slower than other available methods,[14] and the Kutta δ^2 requires more computer memory storage than the widely used Numerov method.[12,14]

The angular momentum coupling scheme used in this model is the usual LS coupling of the Russell-Saunders analysis.[15] The subshells are assigned a rank according to the equation

$$s=n(n-1)/2+l+1\ . \tag{12}$$

The total orbital and spin angular momenta of the two subshells with the lowest rank (smallest s's) are coupled together, and the resultant orbital and spin angular momenta are coupled to the totals of the next-higher subshell, etc. Eventually, when all subshells have been considered, the total orbital and spin angular momenta of the multiplets of interest have been generated. While the radial orbitals for the Rydberg and continuum electrons are computed in the average configuration approximation, the total wave function is constructed to be an antisymmetric eigenfunction of the spin angular momentum and of the orbital angular momentum.

The autoionizing rate is computed as the square of the matrix element of the Coulomb interaction taken between the continuum state and the autoionizing state,[5-7]

$$A_a(j;i\varepsilon_j)=\sum_{i'}\left|\left\langle j\left|\frac{1}{r_{ii'}}\right|i\varepsilon_j\right\rangle\right|^2\ . \tag{13}$$

The Coulomb matrix element itself is a summation of Slater integrals, and is of the form

$$|\langle j\,|\,r^{-1}\,|\,i\varepsilon_j\rangle\,|=\sum_k c_kR^k(n_1l_1,n_2l_2,n_3l_3,n_4l_4)\ , \tag{14}$$

where the Slater integral $R^k(1,2,3,4)$ is defined in the usual manner with each (n_il_i) indicating one of the core, Rydberg, or continuum orbitals, as is appropriate, and the coefficients c_k are the Slater coefficients arising from the analysis of the angular momentum coupling.[16,17] The radiative transition rate $A_r(j;k)$ is computed as the usual dipole transition rate. While forbidden radiative transitions have not been considered as potential radiative stabilizing transitions in this work, all possible autoionizing transitions, nondipole as well as dipole allowed, are included.

In summary, the atomic structure and collision process used in the computations of the dielectronic recombination coefficients described here are modeled by isolated and narrow autoionizing resonances, single configurations, Russell-Saunders LS coupling, frozen atomic cores, local exchange, and distorted waves. External fields and the modifications of the atomic structure and of the excited-state populations of the ion by collisions with other plasma constituents have not been considered. This model should be quite adequate for the computation of the rate coefficients for the dielectronic recombination of heavy-ion impurities in the ionization stages which occur in the interiors of tokamak plasmas and in many astrophysical plasmas.

III. CALCULATIONS

The model of the atomic structure and the atomic processes described above has been translated into a set of computer codes designed for large-scale, unmonitored production calculations. The ion (core) wave functions

are computed using either Weiss's code,[9] which is an extension of Clementi's implementation of Roothaan's analytic SCF technique,[8] or Froese-Fischer's numerical Hartree-Fock code.[18] Occasionally, the numerical wave functions are fit to a series of analytic Slater-type orbitals[19] when an analytic representation of the core wave function is needed for special purposes. The differential equations for the bound and continuum orbitals [Eqs. (5)—(11)] are integrated by the Kutta δ^2 method[12] over a logarithmic mesh until the step size reaches a specified size, and then over a linear mesh until the potential term becomes Coulombic. Appropriate inward and outward integration techniques are utilized in order to insure that the integration method remains stable. The bound-orbital solutions are matched, at the point where the potential becomes Coulombic, to Whittaker's representation of the confluent hypergeometric function[20] which is regular for an infinite value of the argument. The continuum orbitals are appropriately matched to a linear combination of the regular and irregular Coulomb functions[21] when the potential becomes Coulombic.

The Russell-Saunders *LS*-coupled total wave function for every term of a specified configuration is determined by the production codes through a combination of tables based upon Slater's tabulations[15] and vector coupling based upon the coupling scheme described in Sec. II. The angular coefficients for both the autoionizing and radiative matrix elements are determined by a computer code which carriers out the Racah algebra[16,17] for the recoupling of these wave functions. The code is self-contained computing all the necessary 3-*j*, 6-*j*, and 9-*j* symbols, and using tables or computing all single- and two-particle coefficients of fractional parentage.[22] While the Fortran language in which the code is written is not recursive, the code maintains the internal stacks and pointers necessary for an overall recursive structure. This type of code allows a small program to rapidly carry out the evaluation of the Slater coefficients for even very complex atomic structures without requiring extensive analysis and determination of various quantities before the code is run. Previous calculations have shown that it is necessary to retain all the Slater-Racah terms in the expression for the amplitude for the autoionization process, i.e., retention of only the dipole term [the $k=1$ term of Eq. (14)] can lead to large errors in the computation of autoionizing rates as well as the incorrect omission of some strong autoionizing transitions.

Autoionizing and radiative stabilizing rates are computed for each autoionizing state of every possible *LS* symmetry arising from all the Rydberg orbitals built upon a specified core state. These core states for the continuum orbitals include not only the states of the ground configuration of the initial ion which are necessary for the computation of the radiationless capture rate of the plasma electron, but, also, the excited core states, such as those defined in Eqs. (3) and (4), which, when energy considerations allow, give rise to autoionizing rates which must be included in the radiative branching ratio appearing in the dielectronic-recombination-coefficient expression of Eq. (1). These rates can have a significant effect upon the dielectronic-recombination coefficient of some atomic structures and lead to the resonance structures which appear in some electron-impact excitation and the ionization cross sections.[23] Doubly excited states which are below the first ionization limit are included as bound, final states for the radiative stabilization transitions and as continuum core states when the atomic structure and energy considerations permit. Radiative stabilizing transitions of autoionizing states in which the more excited (Rydberg) electron makes the transition while the core electron remains in its initial state are included. These transitions occasionally dominate the recombination process for some Rydberg series.

All the matrix elements for the autoionizing and radiative rates computed as described above have a consistent phase. They are stored and will be used when configuration interaction and intermediate coupling are included in the production codes. The wave functions are so easily and quickly generated in the approximations described above that they are not stored.

Rather than compute directly all the rates up to the very high principal quantum numbers of the Rydberg orbitals which are necessary for the determination of coefficient of the total rate of dielectronic recombination of an ion, the known asymptotic properties of the quantum defect, of radiative transition rates, and of autoionizing transition rates have been exploited. Explicit integration of the differential equations for the bound and continuum orbitals [Eqs. (5)—(11)] and direct computation of the autoionizing and radiative rates are carried out for the lower members of every Rydberg series based upon every core state of the initial ion. The determination of the quantum defects, the autoionizing rates, and the radiative rates for higher states of each Rydberg series are carried out by extrapolation. The quantum defects are computed from the energy ε_{nl} determined in solving the bound-orbital Schrödinger equation, Eq. (5), using the usual equation to define the quantum defect,

$$\varepsilon_{nl}=-\left[\frac{z}{n-\mu(\varepsilon)}\right]^2 . \tag{15}$$

The last several quantum defects are used in a least-squares fit to the following polynomial in the energy:

$$\mu(\varepsilon)=\mu_0+\sum_i \mu_i \varepsilon^i . \tag{16}$$

A linear fit is usually sufficient. The quantum defects are well approximated by a simple polynomial because the basic description of the atomic states used in these calculations is the single-configuration model. Configuration interaction with other autoionizing or bound states which would prevent the representation of the quantum defect by a simple polynomial is discussed below. The configuration interaction with the continuum as described originally by Fano[17] is the dielectronic-recombination process discussed in this work.

A similar approach is used to fit the autoionizing amplitudes. The well-known $\nu^{-3/2}$ dependence upon the effective principal quantum number ν of the Rydberg autoionizing orbital is removed from the autoionizing amplitude, and the remainder is fit by the least-squares method

to a polynomial which is reciprocal in powers of ν,

$$\sum_{i'}\left|\left\langle j\left|\frac{1}{r_{ii'}}\right|i\varepsilon_j\right\rangle\right|=c_2\nu_j^{-3/2}\left[1+\sum_m a_m/\nu_j^m\right]. \quad (17)$$

The coefficients c_2 and a_m are determined by the least-squares fit.

The extrapolation of the radiative transitions was obtained by fitting the last several transitions of a series to a formula introduced by Burgess and Seaton[24] which they based upon data generated by Bates and Damgaard[25] using the Coulomb method,

$$\langle j\mid r\mid k\rangle=c_1\frac{\nu_k^2}{\nu_j^{3/2}}\left[1-\left[\frac{\nu_k}{\nu_j}\right]^2\right]^{-\gamma}\times\cos\left[\pi\left[\nu_k-\nu_j+\chi+\frac{\nu_k/\nu_j^2}{1-\nu_k/\nu_j^2}\alpha+\frac{(\nu_k/\nu_j)^2}{1-(\nu_k/\nu_j)^2}\beta\right]\right]. \quad (18)$$

Generally, the cosine can be set to unity and the coefficients c_1 and γ determined by a linear least-squares fit. Inclusion of the cosine term necessitates a nonlinear least-squares fit, and generally does not improve the accuracy for any particular Rydberg series, but does introduce regularity in c_1 and γ.

The coefficients for the rates of dielectronic recombination through the individual members of a particular Rydberg series of autoionizing states are computed, starting with the lowest and proceeding toward the higher states, with a cumulative coefficient maintained. The computation of the coefficient of the total rate for the Rydberg series is terminated when the relative change due to the addition of the cumulative coefficient of ten members of the series to the total coefficient is less than 0.0001.

The dielectronic-recombination rate coefficients for the initial ions Ne^{7+}, Ar^{15+}, Fe^{23+}, and Kr^{33+} of the lithium isoelectronic sequence have been computed using the computational methods described above. When the autoionizing Rydberg orbitals are based upon the core states described in Eqs. (2)—(4), and when the appropriate angular momentum coupling is introduced, the autoionizing states have the form

$$1s^2n_il_inl\,^1L \text{ or } 1s^2n_il_inl\,^3L, \quad (19)$$

where $n_i=2$, 3, or 4. Similarly, the initial continuum states have the form

$$1s^22s\varepsilon l\,^1L \text{ or } 1s^22s\varepsilon l\,^3L, \quad (20)$$

and

$$1s^22p\varepsilon l\,^1L \text{ or } 1s^22p\varepsilon l\,^3L, \quad (21)$$

additional continuum states have the form,

$$1s^2n_il_i\varepsilon l\,^1L \text{ or } 1s^2n_il_i\varepsilon l\,^3L, \quad (22)$$

where $n_i=2$, 3, or 4, and the bound final states have the form

$$1s^22sn'l'\,^1L \text{ or } 1s^22sn'l'\,^3L, \quad (23)$$

TABLE I. The principal quantum numbers for the lowest-lying autoionizing states n_0 and for the highest with directly computed rates n_x based upon the ion core $1s^22p\,^2P$.

Ion	n_0	n_x
Ne^{7+}	8	16
Ar^{15+}	10	18
Fe^{23+}	11	20
Kr^{33+}	16	23

and

$$1s^22pn'l'\,^1L \text{ or } 1s^22pn'l'\,^3L. \quad (24)$$

It must be noted that some states of the form $1s^22pnl$, while doubly excited, are below the first ionization limit, and, consequently, are not autoionizing. They are bound states and can serve as the final states in radiative stabilizing transitions. Autoionizing and radiative stabilizing rates are computed for each state of every possible LS symmetry of the configurations summarized in Eqs. (19)—(24) which satisfy the following criteria:

$$3\le n\le 12 \text{ and } 0\le l\le 8 \text{ for } n_i=3,4 \quad (25)$$

and

$$n_0\le n\le n_x \text{ and } 0\le l\le 8 \text{ for } n_i=2, \quad (26)$$

where n_0 and n_x are defined in Table I. Generally, the contribution to the total dielectronic recombination rate coefficient by states with $l>8$ is negligible.

For each ion approximately 20 000 autoionizing rates were directly computed. Approximately 10 000 radiative rates were directly computed. In the computation of the coefficients of dielectronic recombination described above, these directly computed rates were extrapolated to several hundred thousand autoionizing and radiative stabilizing rates for each ion.

IV. RESULTS AND COMPARISONS

The rate coefficients for the total dielectronic recombination of Ne^{7+}, Ar^{15+}, Fe^{23+}, and Kr^{33+} computed by the methods described in Secs. II and III are tabulated in Tables II—V and displayed in Figs. 1—4. Results are presented for the initial ion in either the $1s^22s\,^2S$ state or the $1s^22p\,^2P$ state and for the primary radiative stabilizing transitions having ($\Delta n\neq 0$) and not having ($\Delta n=0$) changes of principal quantum.

Comparison with rate coefficients computed by other detailed methods are shown in Tables VI—IX. Comparison with various versions of the Burgess-Merts analytic formula are made in Sec. V. The data labeled "Summers" in Tables VI—VIII were computed using the interpolation formulas which Summers derived from his explicitly computed data[26,27] with the contribution by direct radiative recombination removed. The data labeled "McLaughlin and Hahn" for Ar^{15+} in Table VII was taken from their graphically presented data,[28] and the data for Fe^{23+} in Table VIII was parabolically interpolated from their tabular data.[29] The data labeled "Jacobs, Davis, Rogerson,

and Blaha" for Ne^{7+} in Table VI was interpolated from their tabular data.[30] The data labeled "Jacobs, Davis, Kepple, and Blaha" for Fe^{23+} in Table VIII was computed from the analytic fit provided by Woods, Shull, and Sarazin[31] to their tabular data[32] with direct radiative recombination contribution removed. A direct comparison for some of the details of the present calculation with those of McLaughlin and Hahn is made in Table IX. This data was taken from their published work.[28,29]

The detailed computation described in this paper has some aspects similar to the McLaughlin and Hahn calculation[29] of the total dielectronic-recombination rate coefficient for Fe^{23+}. They compute a set of autoionizing and radiative rates as well as the radial orbitals in a configuration-averaged scheme (the "angular-momentum-averaged" procedure), and determine an approximate dielectronic-recombination rate coefficient using these rates. They note the most important recombination paths, and recalculate the autoionizing and radiative rates for these paths using an explicit LS angular momentum coupling scheme. An average of the proportionality factors between the dielectronic-recombination rate coefficients computed for the same paths in the two approximations is determined. The total dielectronic-recombination rate coefficient is computed by multiplying the total rate coefficient computed using the averaged scheme by the average proportionality factor. An additional factor which attempts to approximate the effects of cascades is also included, but for this isoelectronic sequence it is of little consequence. McLaughlin and Hahn computed the continuum orbitals by a distorted-wave technique and the bound orbitals by a Hartree-Fock method. The autoionizing and radiative rates for the $\Delta n=0$ transitions were determined by quantum-defect extrapolations. A slight difference exists between the LS-coupling scheme used here (described in Sec. II) and that employed by

TABLE II. The dielectronic-recombination coefficient for Ne^{7+} for initial ion states $1s^2 2s\ ^2S$ and $1s^2 2p\ ^2P$ and primary radiative stabilizing transitions $\Delta n=0$ and $\Delta n\neq 0$.

	Dielectronic-recombination rate coefficient (10^{-12} cm^3/sec)		
Temperature (keV)	$1s^2 2s\ ^2S$ $\Delta n=0$	$1s^2 2s\ ^2S$ $\Delta n\neq 0$	$1s^2 2p\ ^2P$ $\Delta n\neq 0$
0.005	35.1		0.0210
0.006	37.8		0.0692
0.007	39.3	0.0144	0.158
0.008	39.8	0.0320	0.286
0.009	39.7	0.0589	0.449
0.01	39.0	0.0951	0.639
0.02	27.0	0.802	3.12
0.03	18.6	1.75	5.73
0.04	13.6	2.55	7.61
0.05	10.5	3.07	8.64
0.06	8.35	3.35	9.06
0.07	6.86	3.46	9.10
0.08	5.76	3.46	8.91
0.09	4.93	3.40	8.59
0.10	4.28	3.29	8.22
0.20	1.63	2.09	4.90
0.30	0.908	1.39	3.19
0.40	0.597	0.999	2.27
0.50	0.430	0.759	1.71
0.60	0.329	0.601	1.35
0.70	0.262	0.491	1.10
0.80	0.215	0.411	0.917
0.90	0.180	0.350	0.780
1.00	0.154	0.303	0.674
2.00	0.0550	0.114	0.252
3.00	0.0300	0.0633	0.139
4.00	0.0195	0.0415	0.0914
5.00	0.0140	0.0299	0.0658
6.00	0.0106	0.0228	0.0502
7.00		0.0182	0.0400
8.00		0.0149	0.0328
9.00		0.0125	0.0275
10.00		0.0107	0.0235

TABLE III. The dielectronic-recombination coefficient for Ar^{15+} for initial ion states $1s^2 2s\ ^2S$ and $1s^2 2p\ ^2P$ and primary radiative stabilizing transitions $\Delta n=0$ and $\Delta n\neq 0$.

	Dielectronic-recombination rate coefficient (10^{-12} cm^3/sec)		
Temperature (keV)	$1s^2 2s\ ^2S$ $\Delta n=0$	$1s^2 2s\ ^2S$ $\Delta n\neq 0$	$1s^2 2p\ ^2P$ $\Delta n\neq 0$
0.02	45.7	0.0403	0.267
0.03	38.0	0.299	1.38
0.04	30.6	0.736	2.81
0.05	24.9	1.22	4.13
0.06	20.7	1.71	5.32
0.07	17.5	2.22	6.40
0.08	15.0	2.74	7.43
0.09	13.0	3.26	8.41
0.10	11.5	3.77	9.33
0.20	4.63	6.98	14.1
0.30	2.63	7.27	13.8
0.40	1.75	6.63	12.2
0.50	1.27	5.85	10.5
0.60	0.974	5.12	9.10
0.70	0.778	4.49	7.92
0.80	0.639	3.97	6.95
0.90	0.538	3.53	6.16
1.00	0.461	3.16	5.49
2.00	0.165	1.39	2.37
3.00	0.0902	0.813	1.38
4.00	0.0587	0.548	0.927
5.00	0.0421	0.401	0.677
6.00	0.0320	0.309	0.522
7.00	0.0254	0.248	0.418
8.00	0.0208	0.205	0.345
9.00	0.0175	0.173	0.290
10.00	0.0149	0.148	0.249
20.00	0.00528	0.0535	0.0899
30.00		0.0293	0.0493
40.00		0.0191	0.0321
50.00		0.0137	0.0340
60.00		0.0104	0.0175
70.00			0.0139
80.00			0.0114

McLaughlin and Hahn, but that difference is inconsequential to the total coefficient.

As displayed in Table IX, the calculations reported here and those of McLaughlin and Hahn for the $\Delta n \neq 0$ radiative stabilizing transitions with the initial ion state being the $1s^2 2s\ ^2S$ ground state are quite different. A portion of the difference between the $\Delta n = 0$ calculations comes from the termination in this calculation of the angular momentum values for the autoionizing states larger than eight. This error is only of the order of 20%. The cause of the larger differences between the two calculations when the initial ion is in the $1s^2 2s\ ^2P$ state are not readily apparent. However, if, in the calculations reported here, all radiative transitions from autoionizing states based upon the $1s^2 3ln'l'$ and $1s^2 4ln'l'$ configurations to the states of the $1s^2 2pn''l''$ configurations are incorrectly treated as stabilizing (recombining) transitions, rather than just those to states with energy below the first ionization limit ($n'' < n_0$ of Table I), the McLaughlin and Hahn results are reproduced to within a few percent. Also, the proportionality factor which McLaughlin and Hahn use for this case is large, and it may well be that the accuracy of the McLaughlin and Hahn scaling method decreases if this factor is large.

Somewhat similar calculations for Ar^{15+} were carried out by McLaughlin and Hahn.[28] However, a new proportionality factor was not computed, i.e., they used the same factor in these computations that was determined for Fe^{23+}, arguing that over the range of ion charge in this portion of the lithium isoelectronic sequence the factor should be nearly constant. The differences between the McLaughlin and Hahn results and those reported here are somewhat smaller.

TABLE IV. The dielectronic-recombination coefficient for Fe^{23+} for initial ion states $1s^2 2s\ ^2S$ and $1s^2 2p\ ^2P$ and primary radiative stabilizing transitions $\Delta n = 0$ and $\Delta n \neq 0$.

	Dielectronic-recombination rate coefficient (10^{-12} cm^3/sec)		
Temperature (keV)	$1s^2 2s\ ^2S$ $\Delta n = 0$	$1s^2 2s\ ^2S$ $\Delta n \neq 0$	$1s^2 2p\ ^2P$ $\Delta n \neq 0$
0.03	70.0	0.008 66	0.0573
0.04	54.8	0.0709	0.359
0.05	44.2	0.233	1.00
0.06	36.5	0.490	1.89
0.07	30.8	0.807	2.88
0.08	26.5	1.15	3.85
0.09	23.0	1.48	4.74
0.10	20.2	1.80	5.54
0.20	8.22	3.90	9.50
0.30	4.70	4.97	10.7
0.40	3.12	5.42	10.8
0.50	2.27	5.47	10.5
0.60	1.74	5.31	9.87
0.70	1.39	5.05	9.19
0.80	1.15	4.75	8.52
0.90	0.964	4.44	7.88
1.00	0.826	4.15	7.29
2.00	0.296	2.23	3.76
3.00	0.162	1.40	2.33
4.00	0.106	0.977	1.62
5.00	0.0756	0.731	1.21
6.00	0.0576	0.572	0.942
7.00	0.0457	0.464	0.762
8.00	0.0375	0.386	0.633
9.00	0.0314	0.327	0.536
10.00	0.0268	0.282	0.462
20.00	0.009 50	0.104	0.170
30.00	0.005 17	0.0576	0.0939
40.00	0.003 36	0.0377	0.0614
50.00		0.0271	0.0441
60.00		0.0207	0.0337
70.00		0.0164	0.0268
80.00		0.0135	0.0219
90.00		0.0113	0.0184
100.00			0.0157

TABLE V. The dielectronic-recombination coefficient for Kr^{33+} for initial ion states $1s^2 2s\ ^2S$ and $1s^2 2p\ ^2P$ and primary radiative stabilizing transitions $\Delta n = 0$ and $\Delta n \neq 0$.

	Dielectronic-recombination rate coefficient (10^{-12} cm^3/sec)		
Temperature (keV)	$1s^2 2s\ ^2S$ $\Delta n = 0$	$1s^2 2s\ ^2S$ $\Delta n \neq 0$	$1s^2 2p\ ^2P$ $\Delta n \neq 0$
0.05	63.0		0.0168
0.06	53.5	0.0192	0.0701
0.07	46.0	0.0576	0.188
0.08	40.1	0.128	0.382
0.09	35.3	0.233	0.652
0.10	31.3	0.370	0.982
0.20	13.3	2.21	4.61
0.30	7.74	3.35	6.43
0.40	5.19	3.97	7.26
0.50	3.79	4.33	7.65
0.60	2.92	4.53	7.81
0.70	2.34	4.62	7.81
0.80	1.93	4.62	7.70
0.90	1.63	4.57	7.52
1.00	1.39	4.48	7.29
2.00	0.503	3.13	4.87
3.00	0.275	2.19	3.36
4.00	0.179	1.62	2.46
5.00	0.129	1.25	1.90
6.00	0.0980	1.01	1.52
7.00	0.0779	0.830	1.25
8.00	0.0638	0.699	1.05
9.00	0.0535	0.599	0.899
10.00	0.0457	0.521	0.781
20.00	0.0162	0.200	0.298
30.00	0.008 81	0.1123	0.167
40.00	0.005 73	0.0737	0.110
50.00	0.004 10	0.0531	0.0790
60.00	0.003 12	0.0407	0.0604
70.00	0.002 47	0.0324	0.0481
80.00		0.0266	0.0395
90.00		0.0223	0.0332
100.00		0.0191	0.0284

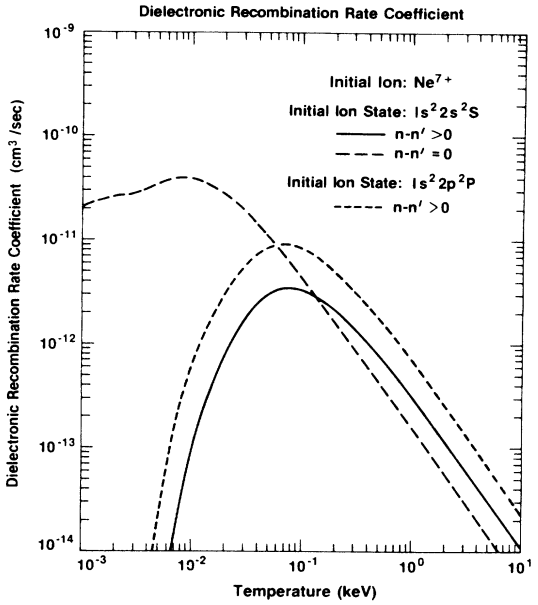

FIG. 1. Detailed calculation of the rate coefficient for the dielectronic recombination of Ne^{7+} in a low-density plasma.

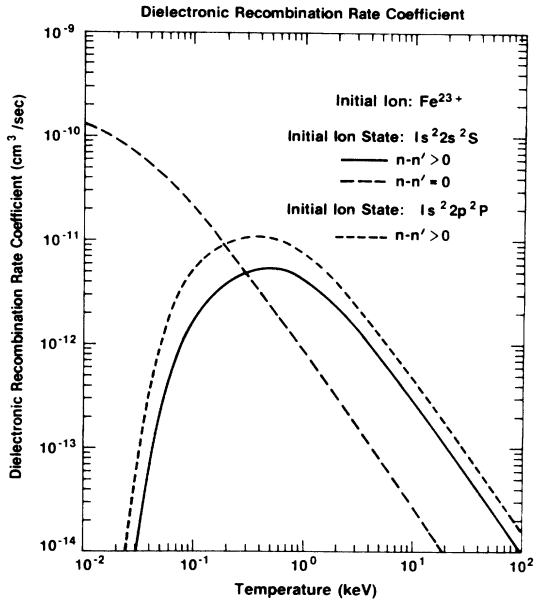

FIG. 3. Detailed calculation of the rate coefficient for the dielectronic recombination of Fe^{23+} in a low-density plasma.

The Ne^{7+} coefficients (Table VI) of Jacobs, Davis, Rogerson, and Blaha[30] and the Fe^{23+} coefficients (Table VIII) of Jacobs, Davis, Kepple, and Blaha[32] use autoionizing rates computed by a quantum-defect extrapolation into the negative-energy region of partial-wave excitation cross sections computed at threshold. Only dipole-allowed excitations from the ground state $1s^2 2s\ ^2S$ (in LS coupling) were considered. A distorted-wave theory was used to compute the excitation cross sections. Apparently a Hartree-Fock method was used to compute the bound orbitals for the radiative transition rates. An LS-coupling scheme similar to McLaughlin and Hahn's was employed. The calculations reported here agree to within a few percent with those of Jacobs, Rogerson, Kepple, and Blaha for Ne^{7+} and those of Jacobs, Davis, Kepple, and Blaha for Fe^{23+} at the lowest temperatures where the $\Delta n=0$ radiative stabilizing transitions dominate, but are approximately 50% larger at the higher temperatures where the

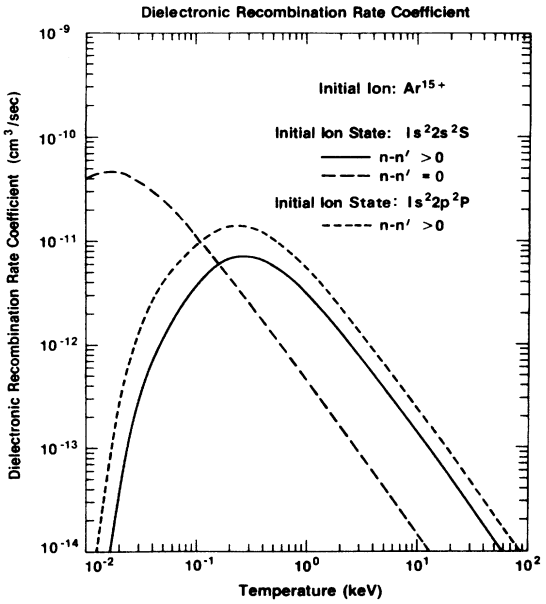

FIG. 2. Detailed calculation of the rate coefficient for the dielectronic recombination of Ar^{15+} in a low-density plasma.

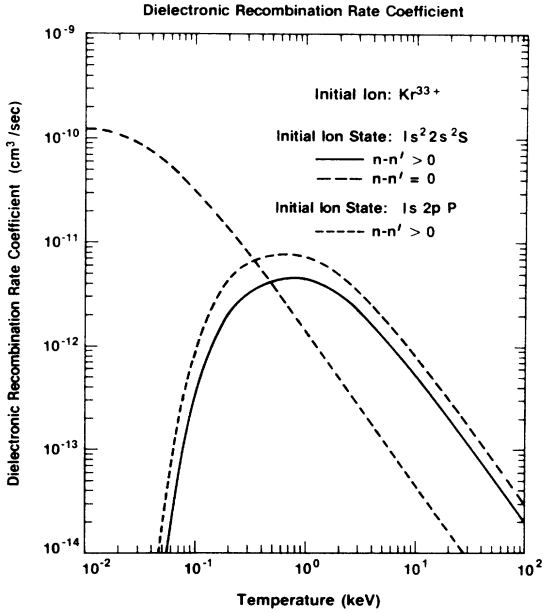

FIG. 4. Detailed calculation of the rate coefficient for the dielectronic recombination of Kr^{33+} in a low-density plasma.

TABLE VI. Comparison of the dielectronic-recombination coefficient for Ne^{7+} computed by several different methods for the initial ion state $1s^22s$ with all radiative stabilizing transitions.

Temperature (keV)	Dielectronic-recombination rate coefficient (10^{-12} cm^3/sec) Roszman	Jacobs, Davis, Rogerson, and Blaha	Summers
0.008	39.8	33.9	
0.01	39.1	35.7	
0.05	13.6	11.1	27.2
0.10	7.57	4.80	23.3
0.50	1.19	0.951	5.39
1.00	0.457		2.18
2.00	0.169		0.862

$\Delta n \neq 0$ transitions dominate. Similar ranges of agreement and disagreement occur when comparison is made for the coefficients of other elements in the lithium isoelectronic sequence which have been computed by Jacobs, Davis, and co-workers[30–35] with coefficients computed using an interpolation procedure for the detailed coefficients reported here (discussed in Sec. V). The autoionization into excited states with the same principal quantum number of the excited electron as that of the core-excited electron of the autoionizing state, a process which has been emphasized by Jacobs, Davis, and co-workers, has been included in the calculations reported here. The modification of the dielectronic-recombination rate coefficients by these extra autoionization channels for highly charged ions which are members of the lithium isoelectronic sequence is generally small since the less-excited Rydberg autoionizing states which contribute most to the dielectronic recombination lie below the threshold for these channels. As an example, for Fe^{23+} only states from the configurations $1s^23pnl$ with $n \geq 24$ can autoionize into the continuum $1s^23s\varepsilon l'$. A significant departure from this model occurs for the less highly charged ions such as Ne^{7+}. This departure is discussed in Sec. V. The major difference between the atomic model used by Jacobs, Davis, and co-workers and that of the work reported here is the exclusion by Jacobs, Davis, and co-workers of the nondipole excitations to configurations $1s^23snl$ and $1s^23dnl$ in the radiationless capture process and either the subsequent decay by radiative transitions into the bound, doubly excited states of the configurations $1s^22pn'l'$ or the decay of nondipole autoionization into other energetically possible excited states. The rate coefficients of Jacobs, Davis, and co-workers for Fe^{23+} can be reproduced to within 10% from the detailed calculations reported here when only dipole-allowed autoionizing transitions are included. A similar calculation for Ne^{7+} produces rates within 20% of the Jacobs, Davis and co-workers rates. While the extrapolation procedure likely is not accurate for the lower members of the various autoionizing Rydberg series which are important for Fe^{23+}, as discussed in Sec. V, the error introduced into the calculation of the total rate does not appear to be large. Of course, this method also depends upon the accuracy of the partial-wave-excitation cross sections. These are not available for examination.

Summers in his large-scale ionization equilibrium calculations[26,27] used the original Burgess analytic expression[3,4] for the rate coefficient of dielectronic recombination with the oscillator strengths computed in the Coulomb approximation. The agreement between the data reported here and Summers's for Ne^{7+}, Ar^{15+}, or Fe^{23+} is not very good since Summers's data differs only slightly from coefficients computed using the original Burgess analytic formula with oscillator strengths computed in the Hartree-Fock approximation. As noted by Merts, Cowan, and Magee,[1] this is not a good approximation in the temperature region where radiative stabilizing transitions of the type $\Delta n \neq 0$ dominate. For Fe^{23+} the Summers's data is somewhat larger than the Burgess data which probably reflects the error in extrapolation to outside the region where data was actually calculated. The Ne^{7+} and Ar^{15+} coefficients were obtained by the spline interpolation suggested by Summers and are within the region where data was computed.

These comparisons demonstrate that when the regions of validity of even simple atomic models overlap (such as the low-temperature region) with the more exact and detailed model defined in Sec. II, the agreement between the total dielectronic-recombination rate coefficients is quite good. However, models which oversimplify the atomic structure, neglect important atomic processes, and the energy selection rules of various processes cannot yield accurate dielectronic-recombination rate coefficients and must be used with extreme caution.

TABLE VII. Comparison of the dielectronic-recombination coefficient for Ar^{15+} computed by several different methods for the initial ion state $1s^22s$ with all radiative stabilizing transitions.

Temperature (keV)	Dielectronic-recombination rate coefficient (10^{-12} cm^3/sec) Roszman	McLaughlin and Hahn	Summers
0.10	15.3		20.1
0.50	7.12	7.9	11.1
1.00	3.62	4.3	7.71
2.00	1.56	2.1	3.49
3.00	0.903	1.3	2.15
6.00	0.341		0.813

V. FITTING AND INTERPOLATION OF THE DATA

The relative differences between the coefficients for the total rates related to the $\Delta n \neq 0$ and $\Delta n = 0$ radiative transitions computed as described above, and those computed from the Burgess analytic formula[4] for the $\Delta n = 0$ transitions and with the Merts-Cowan-Magee correction[1] for

TABLE VIII. Comparison of the dielectronic-recombination coefficient for Fe^{23+} computed by several different methods for the initial ion state $1s^22s$ with all radiative stabilizing transitions.

Temperature (keV)	Dielectronic-recombination rate coefficient (10^{-12} cm^3/sec) Roszman	McLaughlin and Hahn	Jacobs, Davis, Kepple, and Blaha	Summers
0.10	22.0		22.8	26.0
0.50	7.74		4.54	17.1
1.00	4.98	8.37	2.67	13.8
3.00	1.56	3.21	0.806	4.94
6.00	0.630	1.11	0.323	2.06

the $\Delta n \neq 0$ transitions (in short, the Burgess-Merts formula) are displayed in Figs. 5–7. The analytic Burgess-Merts formula is the following:[1,4]

$$\alpha(i)=4.782\times 11^{-12}T^{-3/2}B(z)\sum_{i'} f_{ii'}A(x)e^{-E/T}, \quad (27)$$

where

$$B(z)=[z(z+1)^5/(z^2+13.4)]^{1/2}, \quad (28)$$

$$E/T=(z+1)^2(\nu_i^{-2}-\nu_{i'}^{-2})/Ta, \quad (29)$$

with

$$a=1+0.015z^3/(z+1)^2, \quad (30)$$

and

$$A(x)=x^{-1/2}/(1+0.105x+0.015x^2), \quad (31)$$

for the original Burgess expression,[4] or

$$A(x)=0.5x^{1/2}/(1+0.210x+0.030x^2), \quad (32)$$

for the Merts-Cowan-Magee correction[1] with

$$x=(z+1)/(\nu_i^{-2}-\nu_{i'}^{-2}). \quad (33)$$

The quantity $f_{ii'}$ is the absorption oscillator strength for the transition from the ground state i to the excited state i'. The summation over i' is carried out for all transitions of interest. The quantity ν_i is the effective principal quantum number for the state i. The temperature T is in rydbergs.

The relative difference displayed in Figs. 5–7 is defined as the difference between the rate coefficient computed by the detailed method and that computed from the Burgess-Merts analytic formula divided by the detailed rate coefficient. Both unmodified hydrogenic oscillator strengths and oscillator strengths and effective quantum numbers computed in the single configuration, Hartree-Fock approximations[18] were used in computing the rate coefficients with the Burgess-Merts formula for the $\Delta n \neq 0$ transitions. Only the Hartree-Fock data was used for the $\Delta n = 0$ transitions. The data used in these calculations is tabulated in Tables X and XI. The differences between the rate coefficients computed from the Burgess-Merts formula using either the hydrogenic or the Hartree-Fock quantum numbers and oscillator strengths reflect how "hydrogenic" the highly ionized elements of the lithium isoelectronic sequence are.

A brief inspection of Figs. 5–7 reveals that in the asymptotic temperature region [$T > 0.9E$, where E is defined in Eq. (30)] the agreement between the dielectronic-recombination rate coefficients for the ions Ar^{15+}, Fe^{23+}, and Kr^{33+} computed by detailed calculations reported here and those computed using the Burgess analytic expression and the Burgess expression with the Merts-Cowan-Magee correction, Eqs. (27)–(33), is remarkable, being 20% or less. The differences near the temperatures of the peaks of the rate coefficients and in the low-temperature regions are quite large. The rates for Ne^{7+} computed by the two methods are quite different. While the causes for some of these differences have implications for the determination of corrections to the Burgess-Merts expression and for the derivation of alternate analytic expressions for the dielectronic-recombination rate coefficients, any agreement between the dielectronic-recombination rate coefficients computed in a detailed

TABLE IX. Detailed data for this calculation and for that of McLaughlin and Hahn (Ref. 24) for Fe^{23+}.

	Dielectronic recombination rate coefficient (10^{-12} cm^3/sec)								
Ion state	$1s^22s\ ^2S$			$1s^22s\ ^2S$			$1s^22p\ ^2P$		
Δn change	$\Delta n=0$			$\Delta n\neq 0$			$\Delta n\neq 0$		
Temperature (keV)	1.00	2.00	4.00	1.00	2.00	4.00	1.00	2.00	4.00
Roszman	0.826	0.296	0.106	4.15	2.23	0.977	7.29	3.76	1.62
McLaughlin and Hahn	1.67	0.61	0.218	6.62	3.46	1.53	8.59	4.53	2.03

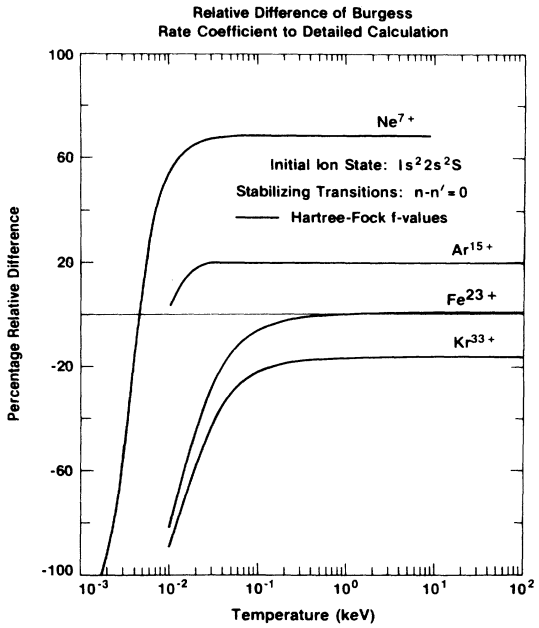

FIG. 5. Relative difference between the rate coefficient for dielectronic recombination computed from the Burgess-Merts formula and that from the detailed calculation for $\Delta n=0$ radiative stabilizing transitions.

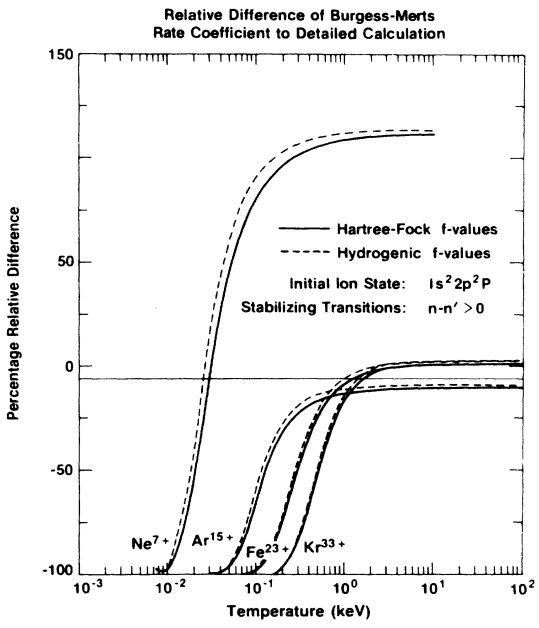

FIG. 7. Relative difference between the rate coefficient for dielectronic recombination computed from the Burgess-Merts formula and that from the detailed calculation for $\Delta n\neq 0$ radiative stabilizing transitions and the initial ion state $1s^2 2p\ ^2P$.

calculation and those computed using the Burgess-Merts analytic formula are, as noted by Merts, Cowan, and Magee,[1] "rather fortuitous." The reasons for regarding any agreement or disagreement as relatively unimportant are the large number of generally incorrect approximations made in the computation of the data bases of the original Burgess[3,4] fit and of the Merts, Cowan, and Magee[1] correction. The major approximations for a low-density plasma which are common to the data bases for both formulas are the following: (1) only dipole-allowed transitions of the less highly excited electron are considered in any radiationless capture or any autoionization; (2) only radiative transitions by the less highly excited electron are included, i.e., no radiative transitions by the more highly excited electron are permitted; and (3) no autoionization into excited states is allowed. Two additional approximations made for the Burgess expression[3,4] are the extrapolation of partial-wave excitation cross sections to below the excitation threshold in order to determine the autoionization rates and the use of hydrogenic cross sections. Two additional approximations used by Merts, Cowan, and Magee[1] were the use of array-averaged autoionization and radiative transition rates.

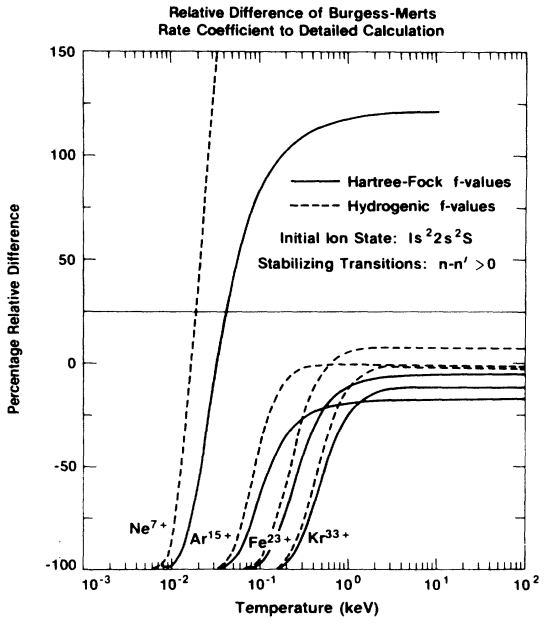

FIG. 6. Relative difference between the rate coefficient for dielectronic recombination computed from the Burgess-Merts formula and that from the detailed calculation for $\Delta n\neq 0$ radiative stabilizing transitions and the initial ion state $1s^2 2s\ ^2S$.

TABLE X. The effective quantum numbers for the outer electron of the lithiumlike ions in various states in the single configuration, Hartree-Fock configuration-averaged approximation.

State	Ne^{7+}	Ar^{15+}	Fe^{23+}	Kr^{33+}
$1s^2 2s$	1.910 18	1.952 22	1.967 45	1.976 72
$1s^2 2p$	1.977 26	1.986 66	1.990 61	1.993 15
$1s^2 3s$	2.913 43	2.954 08	2.968 74	2.977 66
$1s^2 3p$	2.977 09	2.986 76	2.990 73	2.993 27
$1s^2 3d$	2.999 30	2.999 51	2.999 63	2.999 72
$1s^2 4s$	3.914 44	3.954 66	3.969 14	3.977 96
$1s^2 4p$	3.977 06	3.986 80	3.990 77	3.993 30
$1s^2 4d$	3.999 08	3.999 35	3.999 51	3.999 64

TABLE XI. The absorption oscillator strength for the noted transitions in lithiumlike ions and in hydrogen.

Transition	Ne^{7+}	Ar^{15+}	Fe^{23+}	Kr^{33+}	H
$2s$-$2p$	0.1534	0.078 27	0.052 49	0.037 17	
$2p$-$3s$	0.024 47	0.018 72	0.016 94	0.015 92	0.013 59
$2s$-$3p$	0.2992	0.3621	0.3852	0.3993	0.4349
$2p$-$3d$	0.6662	0.6789	0.6841	0.6873	0.6958
$2p$-$4s$	0.004 957	0.003 979	0.003 662	0.003 477	0.003 045
$2s$-$4p$	0.080 43	0.091 48	0.095 23	0.097 45	0.1028
$2p$-$4d$	0.1232	0.1227	0.1225	0.1223	0.1218

As noted in the discussion of Sec. IV concerning the data of Jacobs, Davis, and co-workers the use of autoionizing rates computed in the "dipole-only" approximation is not adequate. Inspection of the autoionization rates computed in the course of the detailed calculation reported here reveals that the nondipole capture transitions (and the corresponding autoionizing rates) from the states of the initial configuration $1s^2 2s\varepsilon l$ to the autoionizing states of the $1s^2 3snl$ and $1s^2 3dnl$ configurations are at least as large and generally larger than the dipole transitions to the states of the $1s^2 3pnl$ configurations. The large radiative transition rates from the $1s^2 3dnl$ configuration states to those states of the $1s^2 2pn'l'$ configuration which are below the first ionization limit cause the nondipole transitions to contribute significantly to the dielectronic-recombination process. This point was also noted by Merts, Cowan, and Magee.[1] The neglect of autoionization into all energetically allowed continua based upon excited configurations, such as the autoionization of $1s^2 3dnl$ into the $1s^2 2p\varepsilon l'$, $1s^2 3s\varepsilon l'$, and $1s^2 3p\varepsilon l'$ continua, can result in the computation of a dielectronic-recombination rate coefficient which is much too large. As noted below, this neglect is most severe for light ions. Additional inspection of the data used here has revealed that radiative stabilizing transitions by the more highly excited electron in some autoionizing states is much larger than those of the less highly excited electron, and, hence, cannot be neglected. The additional approximations have uncertain errors, though it is known that the use of array-averaged transition rates generally yields dielectronic-recombination rate coefficients which are too large.[1]

Several different atomic models which excluded various autoionization and radiative stabilizing channels were constructed in an attempt to determine the dominant processes and to understand the agreement with the Burgess-Merts analytic expression. No less detailed model than the one described in Sec. II was found which would yield accurate dielectronic-recombination rate coefficients over the range of the lithium isoelectronic sequence considered here and over the entire temperature range where the rate coefficients were non-negligible. The failure of a simple model to provide accurate rate coefficients can be understood in terms of a few scaling laws of atomic quantities and of some extrema of several functional forms.

The scaling of the transition rates will be noted first. The strongest radiative transition of an autoionizing state which leads to a stable ground state generally involves the core-excited electron (the less-excited electron). The rate of this transition is essentially constant along a Rydberg series since the more highly excited electron perturbs the core only slightly, but does increase roughly as the fourth power of the effective charge of the initial ion for $\Delta n \neq 0$ transitions and as the first power of the effective charge of the initial ion for $\Delta n = 0$ transitions,[10] i.e.,

$$A_r(j;k) \approx \text{const} \times z^4 \quad (\Delta n \neq 0) \tag{34}$$

and

$$A_r(j;k) \approx \text{const} \times z \quad (\Delta n = 0) , \tag{35}$$

for the entire isoelectronic sequence, where z is the effective charge of the initial ion (before recombination). An autoionizing rate for a particular state decreases as the inverse third power of the principal quantum number of the state,[10] but depends so weakly upon the effective charge of the initial ion that it can be taken to be independent of the charge over large portions of the isoelectronic sequence, i.e.,

$$A_a(j;i\varepsilon_j) \approx \text{const}/n_j^3 , \tag{36}$$

for the entire isoelectronic sequence, where n_j is the effective principal quantum number of the autoionizing state labeled by j.

Next, several extrema of the dielectronic-recombination rate coefficient as defined by Eq. (1) are noted. The temperature T_j for which the rate coefficient for the dielectronic recombination through a particular autoionizing state, labeled by j, has its maximum is defined by the following:

$$T_j = 2\varepsilon_j/3 . \tag{37}$$

Assuming that the autoionizing rates along a Rydberg series can be represented by their asymptotic form, namely,

$$A_a(j,i\varepsilon_j) = a_i/n_j^3 , \tag{38}$$

the coefficient of the thermal exponential in Eq. (1),

$$f(n) = \frac{a_i/n^3 A_r(j;k)}{\sum_{i'} a_{i'}/n^3 + \sum_k A_r(k;j)} , \tag{39}$$

is a monotonically decreasing function which begins to decrease rapidly along the Rydberg series (its second

derivative with respect to n is zero) for n larger than the value of n_x which is determined from the following expression:

$$n_x = \left[\frac{\sum_{i'} a_{i'}}{2 \sum_{k} A_r(k;j)} \right]^{1/3} . \quad (40)$$

For members of the series with principal quantum number n smaller than n_x, the quantity $f(n)$ as defined in Eq. (39) is almost constant. The rate of decrease of $f(n)$ is large once $n > n_x$ if n is small, but is small if n is large. If the energy ε_j is assumed to have a hydrogenic form,

$$\varepsilon_j = (z+1)^2 \left[\frac{1}{\nu_i^2} - \frac{1}{\nu_{i'}^2} \right] - \frac{z^2}{n_j^2} , \quad (41)$$

where ν_i is the effective quantum number of the interacting bound electron in the continuum state of the ion and $\nu_{i'}$ is its effective quantum number in the core-excited state, one can see that the thermal exponential at any temperature is also a monotonically decreasing function of n_j.

The hydrogenic form of the autoionization energy, Eq. (41), can be used to determine, approximately, the minimum principal quantum number of the Rydberg electron n_j at which autoionization into a particular excited core can occur. Since the autoionization energy ε_j will be zero at the threshold for autoionization, all states with principal quantum numbers n_j satisfying the following inequality will autoionize into the continua which has the core state containing an excited electron with effective principal quantum number ν_i:

$$n_j > \frac{z}{(z+1)^2} \left[\frac{1}{\nu_i^2} - \frac{1}{\nu_{i'}^2} \right]^{-1/2} . \quad (42)$$

Generally, because the autoionization into excited states occurs at small energies ε_j, these rates are as large or larger for all angular momentum values than those rates for autoionization into the ground state.

For weakly charged ions, the radiative transition rates for both the $\Delta n = 0$ and $\Delta n \neq 0$ cases are typically 10^7 to 10^8 transitions/sec and are negligible compared to the autoionizing rates, which are on the order of 10^{14} transitions/sec. The quantity n_x defined in Eq. (40) has a value of $n_x \approx 200$. The rate coefficient for the dielectronic recombination through the state with $n = 400$ will be roughly one-third the value for $n = 200$, implying that the convergence is slow. Clearly, for a high temperature, the largest number of autoionizing states contributing to the dielectronic recombination will be close to the large-n limit of Eq. (42),

$$\varepsilon_\infty = (z+1)^2 \left[\frac{1}{\nu_i^2} - \frac{1}{\nu_{i'}^2} \right] . \quad (43)$$

For all autoionizing Rydberg series of weakly charged ions and for the $\Delta n = 0$ series of all ions, n_x is quite large. Autoionization into excited states will occur for small n_j.

For somewhat more highly charged ions n_x is much smaller for the autoionizing $\Delta n \neq 0$ Rydberg series since, because of the effective charge (z) dependence, the radiative rates become comparable to the autoionizing rates for even the lowest members of a series. The dielectronic-recombination rate is largest for the lower members of these series and decreases rapidly for $n_j > n_0$. The analysis of the $\Delta n = 0$ cases for these ions does not change significantly because of the effective charge dependence of the $\Delta n = 0$ radiative transition rates. For very highly charged ions, the radiative rates are much larger than the autoionizing rates for all members of the $\Delta n \neq 0$ series, and the convergence pattern of the total dielectronic-recombination rate is modified accordingly.

Ne^{7+} is essentially an example of the more weakly charged ion case. For Ne^{7+}, $n_x \approx 13$ and the coefficient for $n = 50$ is approximately 5% of the term at n_x. All the states based upon the $1s^2 3l$ and $1s^2 4l$ cores can autoionize into the continua of the $1s^2 2p$ core. For Ne^{7+}, autoionization of the states of the $1s^2 3pnl$ and of the $1s^2 3dnl$ configurations into the continua of the $1s^2 3s\varepsilon l'$ configuration occurs roughly for n larger than 13 and 11, respectively, as computed from Eq. (42), and for O^{+7} for n larger than 11 and 9, respectively. The suppression of the dielectronic recombination will be larger since these autoionizing rates are large. This should account for the larger difference between the rate coefficients computed by the detailed method and those computed from the Burgess-Merts formula for Ne^{7+} as noted in Fig. 5, and for the differences for O^{+5} noted by McLaughlin and Hahn.[28]

Ar^{15+} is a transition case on the moderately charged side. The n_x for Ar^{15+} is $n_x \approx 5$ and the coefficient of $n = 20$ is approximately 5% of the one for $n = 5$. Autoionization into the excited states noted above occurs for n larger than 19 and 16, respectively.

Fe^{23+} and Kr^{33+} are examples of the moderately charged case. The n_x for Fe^{23+} is 2.6 with the coefficient for $n = 10$ being 5% of the one for n_x. The autoionization into the excited states occurs for n larger than 24 and 20, respectively, for Fe^{23+}. The n_x for Kr^{+23} is 1.6, and the $n = 6$ coefficient is 5% of the n_x coefficient. The autoionization into the excited states occurs for n larger than 29 and 24, respectively, for Kr^{33+}. Of course, the n_x values for Fe^{23+} and Kr^{33+} have only mathematical meaning since the Rydberg series does not contain these members. Also, there is no significant suppression of the dielectronic recombination by autoionization into the excited states.

In the single exponential of the Burgess expression the energies of the autoionizing states are approximated by the excitation energy of the stabilizing radiative transition, Eq. (43). This approximation yields nearly the correct asymptotic temperature dependence, approximately $T^{-3/2}$, for all ions. The correct temperature dependence near the peak and in the low-temperature region for any ion cannot be obtained with this choice of functional form and of energy. The low temperatures emphasize the energy and coefficients of the lowest members of a Rydberg series which are not well approximated by any of the asymptotic estimates discussed above. Additionally, the larger differences between the energies of the lowest members of a Rydberg series, which dominate the rate coefficient for the dielectronic recombination of moderately and highly charged ions, indicate that a single

thermal exponential is unlikely to be an adequate representation over the entire energy-temperature region which is of importance. Experience with fitting the computed data to interpolation expressions, which is discussed below, supports this analysis.

The implications of the above analysis are that the scaling of dielectronic recombination with the effective charge of the ion and with the principal quantum numbers of the members of a Rydberg series are too complex for a single thermal exponential representation[34] and for a monolithic functional form for the coefficients of the thermal exponentials. Simple scaling arguments which assume that the functional dependence upon the temperature, the principal quantum number, and the ionic charge are the same for all members of a Rydberg series which have a significant contribution to the coefficient of dielectronic recombination[36] of an ion are not likely to produce useful analytic expressions over the entire temperature range or over a significant portion of the isoelectronic sequence containing the ion.

A procedure which allows the interpolation of the directly computed data described above for the total rates of dielectronic recombination of the lithium isoelectronic sequence and incorporates the implications of the analysis described above has been developed and is presented here. This procedure begins by fitting the total rates for the four ions considered, Ne^{7+}, Ar^{15+}, Fe^{23+}, and Kr^{33+}, to a sum of exponentials,

$$\alpha=\frac{1}{T^{3/2}}\sum_{i=1}^{m} c_i e^{-\xi_i/T} , \tag{44}$$

where the parameters ξ_i are determined by a minimization procedure,[37] and the coefficients c_i by a linear least-squares fit at each minimization step. The minimum number of exponentials required to fit the data of each ion over the temperature ranges 0.01—10 keV for the $\Delta n\neq 0$ transitions was three, i.e., $m=3$, though as one might suspect from the above discussion, two exponentials fit the Ne^{7+} data almost as well as three. For the $\Delta n=0$ transitions over the indicated temperature ranges two exponentials were taken. The parameters ξ_i and the coefficients c_i are tabulated in Tables XII, XIII, and XIV. These fits reproduce the directly computed data to better than 0.01%.

Interpolation of the parameters ξ_i and the coefficients c_i can be carried out by use of the following equations for recombination through the $\Delta n=0$ radiative stabilizing transitions:

$$\log_{10}(c_i)=\sum_{j=1}^{3} a_{ij} z^{j-1} \tag{45}$$

and

$$\xi_i=z^4\sum_{j=1}^{4} b_{ij} z^{1-j} . \tag{46}$$

For recombination through the $\Delta n\neq 0$ transitions, the following equations can be used to interpolate the parameters:

$$\log_{10}(c_i)=\sum_{j=1}^{4} a_{ij}[\log_{10}(z)]^{j-1} , \tag{47}$$

and

$$\xi_i=z^2\sum_{j=1}^{3} b_{ij} z^{1-j} , \tag{48}$$

where, as above, z is the effective charge of the initial ion. The coefficients a_{ij} and b_{ij} are tabulated in Tables XV, XVI, and XVII. These coefficients were determined by a linear least-squares fit. Many different functional forms and methods of fitting the data were tried. These expressions represent the most reasonable compromise between smoothness of fit, accuracy of fit, the simplicity and economy of expression for the lithium isoelectronic sequence. The expressions of Eqs. (44)—(48) cannot be used to extrapolate to either heavier or lighter ions in the lithium isoelectronic sequence since they represent fits of high-order polynomials which diverge and are meaningless outside the data region used in the fit. Additionally, neither the parameters ξ_i nor the coefficients c_i should be compared with the similar-appearing quantities in the Burgess-Merts expressions [Eqs. (27)—(33)] since they represent the rate coefficient for the total dielectronic recombination of the ions in the lithium isoelectronic sequence rather than just the coefficients associated with a particular radiative stabilizing transition.

VI. CONCLUDING REMARKS

The dielectronic-recombination rate coefficients reported here are for ions in the lithium sequence which are several times ionized. The restriction to ions which are several times ionized is based upon a conservative estimate

TABLE XII. The coefficients and parameters for the fit of the exponential series $\alpha=T^{-3/2}\sum_{i=1}^{m} c_i\exp(-\xi_i/T)$ to the directly computed dielectronic-recombination-coefficient when the initial ion is $1s^2 2s\ ^2S$ and the primary radiative transitions have principal quantum-number change $\Delta n=0$

	Ne^{7+}	Ar^{15+}	Fe^{23+}	Kr^{33+}
c_1	5.11×10^{-12}	1.71×10^{-11}	1.71×10^{-10}	2.92×10^{-10}
ξ_1	0.186	0.587	0.587	1.00
c_2	9.13×10^{-11}	2.81×10^{-10}	3.64×10^{-10}	6.18×10^{-10}
ξ_2	1.09	2.04	2.90	3.77

TABLE XIII. The coefficients and parameters for the fit of the exponential series $\alpha = T^{-3/2}\sum_{i=1}^{m} c_i \exp(-\xi_i/T)$ to the directly computed dielectronic-recombination coefficients when the initial ion is $1s^2 2s\ ^2S$ and the primary radiative transitions have principal quantum-number change $\Delta n \neq 0$

	Ne^{7+}	Ar^{15+}	Fe^{23+}	Kr^{33+}
c_1	1.68×10^{-11}	1.86×10^{-10}	7.41×10^{-10}	1.99×10^{-9}
ξ_1	4.16	11.6	22.5	41.2
c_2	1.14×10^{-10}	1.31×10^{-9}	2.07×10^{-9}	4.26×10^{-9}
ξ_2	8.40	28.3	56.0	105.8
c_3	8.49×10^{-11}	1.59×10^{-9}	3.34×10^{-0}	5.99×10^{-9}
ξ_3	10.8	38.3	81.3	160.3

TABLE XIV. The coefficients and parameters for the fit of the exponential series $\alpha = T^{-3/2}\sum_{i=1}^{m} c_i \exp(-\xi_i/T)$ to the directly computed dielectronic-recombination coefficients when the initial ion is $1s^2 2p\ ^2P$ and the primary radiative transitions have principal quantum-number change $\Delta n \neq 0$

	Ne^{7+}	Ar^{15+}	Fe^{23+}	Kr^{33+}
c_1	3.43×10^{-11}	4.08×10^{-10}	1.65×10^{-9}	3.27×10^{-9}
ξ_1	3.29	9.95	20.1	37.7
c_2	1.94×10^{-10}	2.08×10^{-9}	3.20×10^{-9}	6.48×10^{-9}
ξ_2	7.18	26.0	52.8	101.5
c_3	2.46×10^{-10}	2.69×10^{-9}	5.15×10^{-9}	8.41×10^{-9}
ξ_3	9.35	36.0	78.1	156.0

TABLE XV. The coefficients of the least-squares fit to the parameters and coefficients of the three-exponential fit to the directly computed dielectronic-recombination coefficients when the initial ion is in state $1s^2 2s\ ^2S$ and the radiative transitions are $\Delta n = 0$, and where $\log_{10}(c_i) = \sum_j a_{ij} z^{j-1}$, $\xi_i = z^4 \sum_j b_{ij} z^{1-j}$, and z is the effective charge of the initial ion.

	$j=1$	$j=2$	$j=3$	$j=4$
a_{1j}	−12.24	0.136	−0.001 58	
b_{1j}	0.000 0125	−0.000 769	0.0137	−0.0363
a_{2j}	−10.46	0.0702	−0.000 999	
b_{2j}	−0.000 002 53	0.000 185	−0.005 55	0.186

TABLE XVI. The coefficients of the least-squares fit to the parameters and coefficients of the three-exponential fit to the directly computed dielectronic-recombination coefficients when the initial ion is in state $1s^2 2s\ ^2S$ and the radiative transitions are $\Delta n \neq 0$, and where $\log_{10}(c_i) = \sum_j a_{ij} [\log_{10}(z)]^{j-1}$, $\xi_i = z^2 \sum_j b_{ij} z^{1-j}$, and z is the effective charge of the initial ion.

	$j=1$	$j=2$	$j=3$	$j=4$
a_{1j}	−10.16	−5.83	8.00	−2.32
b_{1j}	0.0275	0.324	0.547	
a_{2j}	−30.50	49.61	−38.51	10.16
b_{2j}	0.0694	0.940	−1.58	
a_{3j}	−24.86	32.80	−22.78	5.53
b_{3j}	0.128	0.617	0.178	

TABLE XVII. The coefficients of the least-squares fits to the parameters and coefficients of the three-exponential fit to the directly computed dielectronic-recombination coefficients when the initial ion is in state $1s^2 2p\ ^2P$ and the radiative transitions are $\Delta n \neq 0$, and where $\log_{10}(c_i) = \sum_j a_{ij}[\log_{10}(z)]^{j-1}$, $\xi_i = z^2 \sum_j b_{ij} z^{1-j}$, and z is the effective charge of the initial ion.

	$j=1$	$j=2$	$j=3$	$j=4$
a_{1j}	−5.02	−19.38	20.40	−6.02
b_{1j}	0.0272	0.234	0.319	
a_{2j}	−30.02	49.10	−38.18	10.09
b_{2j}	0.0700	0.797	−1.83	
a_{3j}	−20.79	24.44	−16.64	3.99
b_{3j}	0.127	0.499	−0.407	

of when the atomic model defined in Sec. II is an accurate representation of the actual physical situation. Ions which are less highly ionized require consideration of the effects of core relaxation (the frozen-core model should not be used) since the effective nuclear charge does not produce such a dominant potential for these ions. Because the electron-electron interactions become more important for the weakly charged ions, Hartree-Fock exchange interactions should be used instead of the local potentials considered here. Strong electron-electron interactions also suggest that the complex effects of configuration interaction may be quite important and that orthogonality of the various orbitals must be "forced." Intermediate coupling might change the rate coefficients somewhat from the LS-coupling case by modification of the atomic structure and alteration of the various recombination channels. An additional potential complication is that the autoionizing resonances may overlap and interference between the resonant (dielectronic) and direct (radiative) recombination process may occur.[5,6] In these cases the expressions for the computation of the coefficient of dielectronic recombination is more complicated than that of Eq. (1). For highly charged ions, relativistic modifications of the (initial ion) core states will have some influence upon the potentials produced. Whether the change of the angular momentum coupling scheme from LS coupling to intermediate coupling will have effects which survive the summation over all possible states is unknown and problematic. Recent analysis[38] of the configuration interaction for Fe^{23+}, which has a roughly equivalent effect upon the dielectronic recombination process, showed large modifications in the dielectronic-recombination rate coefficients through individual autoionizing states but only small differences when the coefficients for the rate of total dielectronic recombination were considered.

In order to compute detailed cross sections of the dielectronic-recombination process for even the range of ionization stages considered here, or in order to compute the spectra of satellite lines produced by dielectronic recombination, one must use the more complete description of the atomic physics. For these quantities, the correct positions of the autoionizing states, and, at a minimum, the relative strengths or intensities can be measured.

The omission of the $1s$ (K-shell) excitation is not a serious approximation in the temperature regime for which the lithiumlike charge state for an ion is the dominant charge state.[28–30,32] However, in a very hot, very rapidly recombining, tenuous plasma, dielectronic recombination through the $1s$ excitation channels could become important.

The detailed calculations reported here as well as those discussed in Secs. IV and V are based upon the model of a low-density plasma with no applied external fields. Effects such as the modification of ionization limits, of energy levels, and of atomic states by plasma produced and/or applied external fields and the variation of the population of the autoionizing states by collisions with constituents of the plasma before radiative stabilization can occur will likely alter the rate coefficients for dielectronic recombination in higher-density plasmas and experimental situations. Since the states of the $1s^2 2pnl$ configurations are the most weakly bound, they will most likely be affected first and quite strongly. Whether these environmental effects will increase or decrease the rate coefficient of dielectronic recombination cannot be estimated without additional detailed calculations since the various processes can be of the same size and of opposite influence.

The general conclusion which can be drawn from comparison of the detailed calculations reported here with other calculations and from the analysis of the magnitude of the influences of the various autoionization and radiative channels is that all processes must be included in the atomic model in order to determine accurate dielectronic-recombination rate coefficients. Simplification of the atomic model of the dielectronic-recombination process by neglecting specific processes will lead to the computation of inaccurate rate coefficients in one temperature region or portion of the isoelectronic sequence even though accurate results may be obtained in some other region.

ACKNOWLEDGMENTS

This work was supported by the Office of Fusion Energy of the Department of Energy. Most of the computations were carried out at the National Magnetic Fusion Energy Computing Center.

[1]A. L. Merts, Robert D. Cowan, and N. H. Magee, Jr., Los Alamos Scientific Laboratory Report No. La-6220-MS, 1976 (unpublished).

[2]D. E. Post, J. V. Jenson, C. B. Tarter, W. H. Grasberger, and W. A. Lokke, At. Data Nucl. Data Tables **20**, 397 (1977).

[3]A. Burgess, Astrophys. J. **139**, 776 (1964); Ann. Astrophys. **28**, 774 (1965).

[4]A. Burgess, Astrophys. J. **141**, 1588 (1965).

[5]Larry J. Roszman, in *Physics of Electronic and Atomic Collisions*, edited by Sheldon Datz (North-Holland, Amsterdam, 1982), p. 641.

[6]Bruce W. Shore, Astrophys. J. **158**, 1205 (1969).

[7]D. R. Bates and A. Dalgarno, in *Atomic and Molecular Processes*, edited by D. R. Bates (Academic, New York, 1962), p.

245.
[8]Enrico Clementi and Carlo Roetti, At. Data Nucl. Data Tables **14**, 177 (1974).
[9]A. W. Weiss (private communication).
[10]Robert D. Cowan, *The Theory of Atomic Structure and Spectra,* (University of California Press, Berkeley, 1981), p. 197.
[11]Merle E. Riley and Donald G. Truhlar, J. Chem. Phys. **63**, 2182 (1975); **65**, 792 (1976).
[12]Charlotte Froese, Can. J. Phys. **41**, 1895 (1963).
[13]E. Cicely Ridley, Proc. Cambridge Philos. Soc. **51**, 702 (1955).
[14]J. W. Cooley, Math Comp. **15**, 363 (1961).
[15]John C. Slater, *Quantum Theory of Atomic Structure* (McGraw-Hill, New York, 1960), p. 239.
[16]Giulio Racah, Phys. Rev. **61**, 134 (1942); **62**, 146 (1942); **63**, 171 (1943); **76**, 187 (1949).
[17]U. Fano, Phys. Rev. **140**, A67 (1965).
[18]C. F. Fischer, Comp. Phys. Commun. **14**, 145 (1978).
[19]L. J. Roszman (unpublished).
[20]Lucy Joan Slater, in *Handbook of Mathematical Functions,* Natl. Bur. Stand. (U.S.) Appl. Math. Ser. No. 55, edited by Milton Abramowitz and Irene A. Stegun (U.S. GPO, Washington, D.C., 1966), p. 503.
[21]Milton Abramowitz, in *Handbook of Mathematical Functions,* Natl. Bur. Stand. (U.S.) Appl. Math. Ser. No. 55, edited by Milton Abramowitz and Irene A. Stegun (U.S. GPO, Washington, D.C., 1966), p. 537.
[22]C. D. H. Chisholm, A. Dalgarno, and F. R. Innes, in *Advances in Atomic and Molecular Physics,* edited by D. R. Bates and Immanuel Estermann (Academic, New York, 1969), p. 297.
[23]M. J. Seaton and P. J. Storey, in *Atomic Processes and Applications,* edited by P. G. Burke and B. S. Moiseiwitsch (North-Holland, Amsterdam, 1976), p. 133.
[24]A. Burgess and M. J. Seaton, Mon. Not. R. Astron. Soc. **120**, 121 (1960).
[25]D. R. Bates and A. Damgaard, Philos. Trans. R. Soc. London A **242**, 101 (1949).
[26]Hugh P. Summers, Appleton Laboratory Internal Memo 367, 1974 (unpublished).
[27]Hugh P. Summers, Mon. Not. R. Astron. Soc. **158**, 255 (1972); **169**, 663 (1974).
[28]D. J. McLaughlin and Yukap Hahn, Phys. Rev. A **29**, 712 (1984).
[29]D. J. McLaughlin and Yukap Hahn, J. Quant. Spectrosc. Radiat. Transfer **28**, 343 (1982).
[30]V. L. Jacobs, J. Davis, J. E. Rogerson, and M. Blaha, Astrophys. J. **230**, 627 (1979).
[31]D. Tod Woods, J. Michael Shull, and Craig L. Sarazin, Astrophys. J. **249**, 399 (1981).
[32]V. L. Jacobs, J. Davis, P. C. Kepple, and M. Blaha, Astrophys. J. **211**, 605 (1977).
[33]V. L. Jacobs, J. Davis, J. E. Rogerson, M. Blaha, J. Cain, and M. Mavis, Astrophys. J. **239**, 1119 (1980).
[34]V. L. Jacobs and J. Davis, Naval Research Laboratory Memorandum Report No. 5105, 1983 (unpublished).
[35]D. Tod Woods, J. Michael Shull, and Craig L. Sarazin, Astrophys. J. **249**, 399 (1981).
[36]Yukap Hahn, Phys. Rev. A **22**, 2896 (1981).
[37]J. A. Nelder and R. Mead, Comput. J. **7**, 308 (1965).
[38]L. J. Roszman and A. Weiss, J. Quant. Spectrosc. Radiat. Transfer **30**, 67 (1983).